Received: 21 December 2022 | Accepted: 20 March 2023

DOI: 10.1002/maco.202213719

ARTICLE

Materials and Corrosion

Characterisation of the galvanic protection of zinc flake coating by spectroelectrochemistry and industrial testing

Florian Feldmann[1,2] | Laura L. E. Mears[1] | Marcel Roth[2] | Markus Valtiner[1]

[1]Institute of Applied Physics, Vienna University of Technology, Vienna, Austria

[2]Dörken Coatings GmbH & Co. KG, Herdecke, Germany

Correspondence
Laura L. E. Mears, Institute of Applied Physics, Vienna University of Technology, Wiedner Hauptstrasse 8-10/E134, Vienna 1040, Austria.
Email: mears@iap.tuwien.ac.at

Abstract

The properties of hot-dip galvanised and electroplated zinc coatings on steel have been widely studied, but the corrosion mechanisms of zinc flake coatings have not yet been investigated in similar detail. Here, we investigate the protective effect of inorganic lamellar zinc coatings, comparing the metallic dissolution rates of different zinc, aluminium and alloyed flakes using an inductively coupled plasma mass spectrometry (ICP-MS) flow cell. These experiments were carried out on both intact and predamaged coatings with different electrolytes. Data were also compared to accelerated laboratory corrosion tests and outdoor weathering results. The chloride concentration, and its effect on the passive oxide film, appears to be a key aspect moderating the dissolution rate and hence sacrificial zinc dissolution under various conditions. The complementary use of accelerated tests and ICP-MS flow cell analysis provides new insights into both the influence of the corrosive environment and the impact of the zinc flake (alloy) used. Based on this approach, tailored coating solutions using zinc flake coatings can be developed.

KEYWORDS

cathodic protection, corrosion protection, thin coatings, zinc lamellar

1 | INTRODUCTION

Zinc is widely used for corrosion protection for steel in many fields. Frequently the application methods used are hot dip galvanising of the steel with molten zinc or electrolytic deposition of zinc and its alloys. In addition to these technologies, zinc flake coatings are increasingly being used in several markets including automotive, renewable energy and construction industries.[1–4]

A striking feature of zinc flake systems is the very low coating thickness (4–20 μm)[5,6] combined with remarkable corrosion protective properties. Due to these thin layers and the associated low demand for raw materials, a high level of material efficiency and sustainable corrosion protection can be realised.[7,8]

Zinc flake technology has many uses in the field of corrosion protection. It is ideal for components for which the standards require high demands on accuracy of fit without rework, like bolts and nuts.[1,9]

Furthermore, this technology is suitable for coating high-strength steels, because the application process does not produce hydrogen, which prevents application-related hydrogen embrittlement of strength classes 10.9 and higher.[10,11]

Figure 1 illustrates the typical structure of a zinc flake coating. They are mainly applied as a modular system

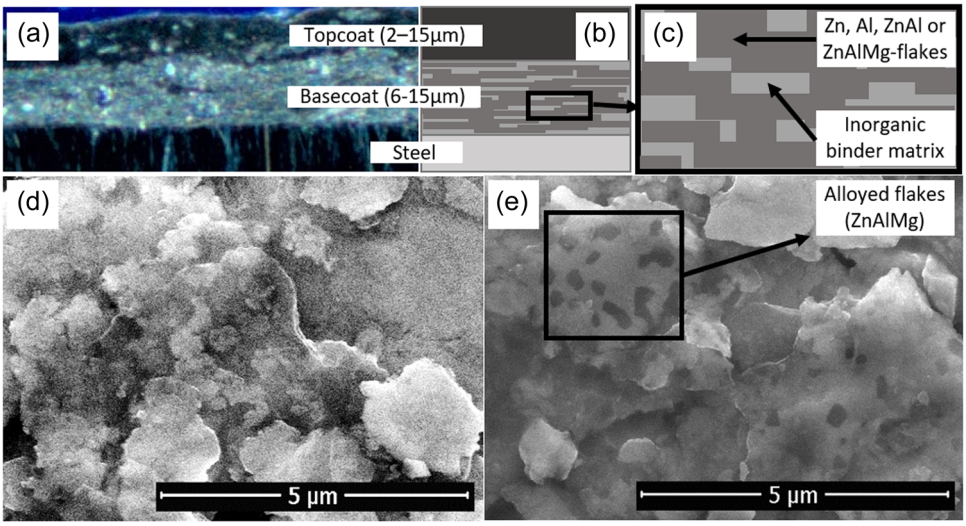

FIGURE 1 (a) Light microscope image (200x) of a zinc flake coating system on a steel sheet with a black topcoat, (b) schematic representation of a typical zinc flake coating system with basecoat and topcoat, and (c) Close up of the base coat schematic, (d) Scanning electron microscope (SEM) picture (20,000x) of a mixed flake system containing zinc and aluminium flakes, (e) SEM picture (20,000x) of a coating containing mainly ZnAlMg flakes and additional zinc flakes and aluminium flakes.

consisting of a basecoat which contains the flakes of zinc, aluminium, ZnAl or ZnAlMg and a further topcoat which has multifunctional aspects such as a defined coefficient of friction, UV- and chemical resistance and colour.[6] In Figure 1a,b, the topcoat is shown to illustrate a typical system. For the later experiments, however, no topcoat was applied to concentrate on the properties of the basecoat. Since zinc performs as a sacrificial anode and actively protects the steel substrate from corrosive attacks, these coatings offer a high level of cathodic protection, which is ensured by the contact network of the single flakes, which are embedded in an inorganic binder matrix. Additional corrosion protection is provided by a passive barrier effect of the coating, therefore, these systems offer a double protection mechanism, which consists of cathodic protection and a barrier function.[12]

Besides the zinc flake systems which are used in this paper, it is also possible to incorporate zinc particles that have spherical or lamellar shapes in organic binder systems (e.g., epoxy systems). These so-called zinc rich primers, of which the above-mentioned zinc flake systems are a subgroup, similarly offer both cathodic protection and a barrier function. Many studies have been published with the scope of finding the best compromise of the cathodic/barrier protection mechanism. Zubielewicz et al. summarise different influences on the performance of zinc-rich primers.[12] To achieve a sacrificial behaviour, it is necessary to have a high amount of active zinc or zinc alloy pigments inside the coating, which is typically at 80 wt%, to guarantee electrical contact between the incorporated zinc pigments. These high pigmentation concentrations over the critical pigment volume concentration (CPVC) can lead, on the other hand, to insufficient mechanical properties of the coating, such as poor adhesion and blister resistance. Further influences on the corrosion resistance of zinc-rich primers are the size and shape (spherical or lamellar) of the pigments, the porosity of the binder, the composition of the used pigments (pure zinc or zinc alloys) and the presence and nature of a further topcoat.[12]

Depending on the respective part geometry, one can choose between different application methods. Bulk goods, such as bolts or nuts, are coated using the dip-spin method, in which a basket containing the parts to be coated is immersed in the coating tank and later centrifuged in a defined manner. Larger parts can also be applied as rack goods in the dip-spin process, by dip-drain or by spraying. After the application, the coating is cured at temperatures between 180°C and 340°C for 20–30 min, which leads to a cross-linking of the titanate-based binding agent.[13,14]

In the automotive industry, accelerated corrosion tests are required to assess the corrosion protection capability of different metals or coatings. These tests are specified in different norms. We can distinguish between constant and cyclical atmospheres which differ from each other concerning the temperature, humidity and the used electrolyte. Accelerated corrosion tests try to simulate corrosion processes in nature in a short time. Hence, materials or components are exposed to test chambers of a corrosive environment (e.g., salt spray) for a certain time and are evaluated afterwards in terms of corrosion protection. It is generally accepted today that

the salt spray test (SST) according to DIN EN ISO 9227 can be used for quality controls. In spite of this, the SST is not capable of simulating the corrosive environment in real life, which is much more complex.[15–17]

Due to the limitations of constant corrosion tests, many automotive companies require a cyclical corrosion test with alternating climate. Compared to the constant climate tests, the environmental conditions change periodically within these tests. These tests are typically recognised as a better approach to the real environment compared to simple constant tests.[15] Table 1 lists various constant corrosion tests and cyclic ageing tests from different original equipment manufacturers (OEMs).

All the aforementioned industrial laboratory corrosion tests accelerate corrosion processes and attempt to predict the real-world corrosion behaviour of metallic components. However, in the case of zinc-coated samples, the complete mechanism of corrosion changes, in accelerated tests, due to the usually high humidity and salt content.[17] Passive layers like zinc carbonates, which build up in the real world[27] and lead to a drastic reduction in the corrosion rate, can no longer form. In the case of hot-dip galvanised samples, for example, the often poor results in salt spray tests can lead to potential misjudgements of the expected performance in outdoor weathering conditions.[28]

Therefore, whether these accelerated tests are able to simulate field exposure conditions has been the focus of research for some time. As an empirical phenomenon, differences in the corrosion protection performance have been observed repeatedly when accelerated tests are compared with outdoor exposure experiments.[29,30]

Hence, currently, outdoor weathering tests are necessary to test the actual behaviour of components and coatings, even if they are significantly more expensive and time-consuming than accelerated tests. Field exposure with zinc-coated steel has been widely investigated over the last decade. To the best of our knowledge, those studies have focused on hot-dip-galvanised and electroplated samples in terms of zinc and its alloys.[31,32] There are hardly any systematic studies in the literature on the correlation of outdoor weathering tests and accelerated corrosion tests of zinc flake systems.

The amount of dissolved zinc allows us to explain the different corrosion results in standardised corrosion tests with different corrosive environments. Higher zinc dissolution measured during inductively coupled plasma mass spectrometry (ICP-MS) experiments may therefore be an indicator of cathodically active behaviour, enabling coating systems to protect steel from corroding in outdoor exposure tests even after applying defined damage to the coating.

In this context, the aim of this paper is to further extend the current knowledge of the performance of zinc flake systems. By using an ICP-MS flow cell, we present an interesting solution to provide new insights into the corrosion mechanism of zinc flake coatings, which will explore the deviating results through methodical electrolyte change in ICP-MS. This will be measured against our hypothesis on the mechanism behind the differing corrosion protection performance.

TABLE 1 Commonly used accelerated corrosion tests in automotive industries with used electrolytes and ranges for temperature (T) and relative humidity (RH).

Standard	T (°C)	RH (%)	Electrolyte
Constant climate tests			
DIN EN ISO 9227 (SST)[16]	**35 ± 2**	–	**5% NaCl (pH = 6.5–7.2)**
DIN EN ISO 6270-2[18]	**40 ± 3**	**100**	**Demineralised water**
Cyclical tests			
VDA 233-102[19]	−15 to 50	50 to 95	1% NaCl (pH = 6.5–7.2)
VW PV 1210[20]	23 to 43	50 to 100	5% NaCl (pH = 6.5–7.2)
VW PV 1200[21]	−40 to 80	30 to 80	–
VW PV 1209[22]	−40 to 80	30 to 80	40 g NaCl+ 10 g $CaCl_2$/l
ACT I[23]	35 to 45	50 to 95	1% NaCl (pH = 4.2)
VCS 1027,1449 (ACT II)[24]	**25 to 50**	**70 to 95**	**0.5% NaCl**
BMW AA-0224[25]	35 to 40	100	5% NaCl (pH = 6.5–7.2)
GMW 14872[26]	20 to 60	≤30 to 100	0.9% NaCl + 0.1% $CaCl_2$ + 0.075% $NaHCO_3$

Note: The specifications highlighted in bold are used in this study.

2 | MATERIALS AND METHODS

2.1 | Chemicals and materials

The chemicals were sourced as follows: sodium chloride from Carl Roth (assay: ≥ 99%); ethanol ≥ 99.9% pure from VWR; technical sodium hydroxide from VWR (assay: 97%); hydrochloric acid from VWR (5N); HNO_3 from VWR; Milli-*Q* water for electrolyte solutions (total organic carbon ≤ 4 ppb, resistivity ≥ 18 MΩ).

For all measurements, S235JR sheets (150 × 75 × 3 mm) were used, which were spray-coated with the different types of zinc flake systems. These sheets were then cured for 30 min at an object temperature of 240°C. The basecoat layers (including the flakes) applied in this way have a thickness of 9–11 μm, which is typical for zinc flake systems. To evaluate the cathodic corrosion protection and to simulate damage to the surface, a scratch was applied to the sheets which goes down to the base metal using a scribe (Erichsen Model 463) with a width of 1 mm. To focus on the behaviour of the zinc flake systems themselves, we have not applied a topcoat for the following experiments.

2.2 | Accelerated corrosion tests

All accelerated corrosion tests have been performed at the facilities of Dörken Coatings GmbH & Co. KG in Germany. As highlighted in Table 1, we executed the salt spray tests (SST) according to DIN EN ISO 9227 (5% NaCl) in a VLM SAL 1000-TL chamber and checked the state of corrosion at the scratched area after 1000 h. The condensed water test, according to DIN EN ISO 6270-2, was carried out in a VLM CON 400-FL and was also checked after 1000 h. For the cyclical corrosion test, we chose the ACT II test according to Volvo VCS 1027,1449 in a VLM CC 1000-FL corrosion chamber. This test consists of (A) a wet phase at room temperature for 6 h with intermittent exposure to 0.5% NaCl solution, (B) a transition phase for 2.5 h with drying under climate control and (C) a 15.5 h phase with constant temperature and humidity at 50°C and 70% RH. These three test phases are repeated from Mondays to Fridays and are followed by a 48-h weekend phase under continued constant climate control (50°C; 70% RH).[24]

2.3 | Outdoor exposure tests

Outdoor exposure tests were performed in two different locations with varying climates. The chosen places are a rural climate in Herdecke, Germany and an urban climate on a rooftop in Vienna, Austria. For each tested coating system, we have assembled four coated S235JR panels (150 × 75 × 3 mm) onto a PVC rack. One out of those four panels had an ideal and nondamaged coating system while the other three panels had scratches with 1 mm width. The PVC racks are safely fixed to the ground by a steel scaffold and are facing south, tilted at a 45° angle. To avoid water accumulation in the crevices, all scaffolds have holes at the corner of the contact regions with the panels.

2.4 | Scanning electron microscopy (SEM)

We carried out the SEM analyses using facilities at the University Service Centre for Transmission Electron Microscopy, Vienna University of Technology, Austria. The SEM was a field emission gun scanning electron microscope (FEG-SEM) Quanta 200F. 1 × 1 cm pieces of zinc flake-coated steel panels were cut and then cleaned in ethanol to remove dust or residues from the surface. Before the measurements, we glued those samples with conductive silver (G302 from Plano) onto a sample carrier. The SEM worked in a fine vacuum of 0.3 mbar. Acceleration voltage was set to 15 kV and the working distance was at circa 7 mm.

2.5 | ICP-MS

ICP-MS measurements were performed using an Agilent 7900 ICP-MS from Agilent Technologies. The calibration was performed with a multielement standard 2A from Agilent Technologies. Before each measurement, the electrolyte was purged with compressed and filtered air for 30 min to assure a constant concentration of dissolved oxygen. The ICP-MS uses an argon plasma and a collision cell with helium as a cell gas and a flow of 5 mL/min. The electrolyte (MilliQ water, 1 mM NaCl or 80 mM NaCl solution) which flows through the electrochemical cell is mixed afterwards with a standard solution. The selfbuilt electrochemical cell, out of PEEK and PTFE, is based on the Ogle- and Mayrhofer designs[33–35] and can also be found in the work of Dworschak et al.[36]. At the beginning of each measurement, the electrolyte flows through a bypass and is diverted after about 2 min through the ICP-MS flow cell with the coated sample to investigate the first seconds of corrosion. The electrolyte is pumped via compressed nitrogen to establish a stable and laminar flow, across the surface of the working electrode in a circular area which is sealed by an O-ring with a diameter of 3 mm. The flow

rate was checked by weighing the collected waste electrolyte and additionally checking the pressure with an in-flow pressure sensor. The samples used were cut panels (1 × 1 cm) of the coated S235JR sheets described earlier. The results and conclusions from the ICP-MS experiments presented in this paper are confirmed by six additional experiments, which were performed in a slightly modified form.

3 | RESULTS AND DISCUSSION

For a visual overview of the morphology of the coating, we first performed scanning electron microscopy of two different test recipes of zinc flake coatings, namely the mixed flake and alloyed flake systems (Table 2a,b).

To understand the corrosion protection performance of the different zinc flake coatings, we have also carried out and compared different accelerated corrosion tests and outdoor weathering studies.

These findings are combined with different ICP-MS tests, for an elemental insight into corrosion with different electrolytes, using a flow cell. Damaged and undamaged steel sheets with different zinc flake systems are measured thus probing local corrosion.

In the following discussion, we will compare four different test recipes of zinc flake systems. The metallic contents of the specific coatings are listed in Table 2. All the listed zinc flake coatings are embedded into an inorganic titanate-based binding matrix as illustrated in Figure 1a–c. Several patents show typical compositions of these titanate-based binder systems.[37,38]

Typical zinc flake systems in the automotive industry often consist of a mix of different flakes (zinc and aluminium).[6] Hence, we start with the mixed and alloyed flake systems (Table 2a,b). In Figure 1d,e, SEM images indicate that the individual flakes in both systems are typically 1–5 μm across and lay on top of each other like scales. The typical thickness of an individual flake is below 1 μm with an aspect ratio (diameter: thickness) of circa 40:1.[39] The contrast in the used flakes is also clearly visible. While the alloyed system shows the alloying elements and different phases, which we see as small dots in the flakes, nothing like this can be seen in the mixed flake system. Due to the inherent size constraints of the zinc flakes and the system they are embedded into, that is surrounded by binder, it is difficult to compare the exact microstructure and the occurring phases within the ZnAlMg flake with other studies,[40,41] to our knowledge these studies are limited to hot-dip galvanised samples. However, the above-mentioned size of the flakes used is in a range where we can assume a high activity, which is also in agreement with other literature that have shown that finer microstructures in ZnAlMg alloys lead to better corrosion protection.[40,41] The following results contribute to our understanding of the working mechanisms of the two different zinc flake systems named in Table 2a,b.

TABLE 2 Metallic contents of the dry zinc flake coatings used in this paper.

Component	Zn content (%)	Al content (%)	Mg content (%)
(a) Mixed flake system			
Zinc flake	70.1	–	–
Aluminium flake	–	7.7	–
ZnAlMg flake	0	0	0
(b) Alloyed flake system			
Zinc flake	14.8	–	–
Aluminium flake	–	4.3	–
ZnAlMg flake	51,4	3,5	3,5
(c) Single flake system (Zn)			
Zinc flake	80.9	–	–
Aluminium flake	–	0	–
ZnAlMg flake	0	0	0
(d) Single flake system (ZnAlMg)			
Zinc flake	0	–	–
Aluminium flake	–	0	–
ZnAlMg flake	71.4	5.4	5.4

Note: The remainder not mentioned in the table consists of inorganic binder (titanates and silicates) and additives (rheological and dispersing).

3.1 | Accelerated laboratory and real-life corrosion tests

Figure 2 shows the results of three different accelerated laboratory corrosion tests, which are (a) SST, (b) constant humidity test and (c) ACT II. Further, in (d and e) two outdoor exposure tests (countryside and city climate) with scratched panels are compared.

Panels a1 and a2 show that especially in the salt spray test, the mixed and alloyed system (Table 2a,b) behaves completely differently. On the one hand, we see in a1 white rust formation on the complete panel with the mixed coating system. In contrast to this, the alloyed zinc flake

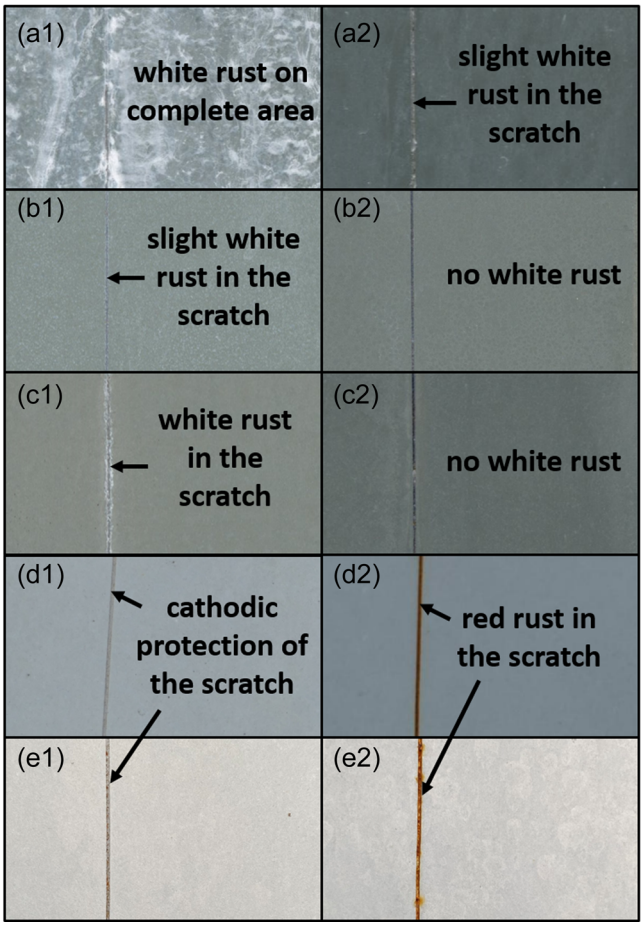

FIGURE 2 Corrosion results with a mixed zinc flake system (left column a1–e1) and an alloyed zinc flake system (right column a2–e2) after different corrosive loads. a1/a2: after 1000 h salt spray test according DIN EN ISO 9227; b1/b2: After 1000 h humidity test according DIN EN ISO 6270-2; c1/c2: after six cycles (6 weeks) ACT II test according VCS 1027,1449; d1/d2: after 6 months of outdoor exposure in Vienna (Austria); e1/e2: after 6 months of outdoor exposure in Herdecke (Germany).

system in a2, with mainly ZnAlMg alloy flakes, shows a more passive behaviour without building up visible corrosion products at the intact area and only very slight white rust in the scratch. This white rust resistance is often required by the automotive industry. We only observe a slight change in colour towards a darker appearance.

Panels b1 and b2 display a second test in a constant climate according to DIN EN ISO 6270-2, which creates an atmosphere of 100% relative humidity at 40°C. Due to the lack of salt in the electrolyte and the corresponding low conductivity, we are facing a completely different appearance of both coating systems after 1000 h inside the corrosion chamber. We cannot see white rust in the intact area, independent of the coating system. In b1, the mixed system only shows minor zinc corrosion products in the scratch.

Panels c1 and c2 are the results for an exemplary cyclical corrosion test which is required in the automotive industry from Volvo Cars (VCS 1027,1449). Cyclical tests are characterised by changing environmental conditions. Inside the applied scratch, we can observe in c1 white rust for the mixed zinc flake but no white rust for the alloyed zinc flake sample in c2.

Panels d1, d2, e1 and e2 compare the previously mentioned results with 6 months of outdoor exposure in an urban climate in Vienna (d1 and d2) and rural climate in Herdecke (e1 and e2). It is fundamental to note that we see critical distinctions in the cathodic corrosion protection of the scratched areas. The mixed coating system with pure zinc and aluminium flakes is still able to protect the scratch (d1 and e1) while the alloyed system with mainly ZnAlMg-flakes is not able to build up a sacrificial protection of the damaged region, which results in the formation of red rust (d2 and e2). The comparison between the corrosion results in the SST (1.5 months) and outdoor exposure trials emphasises once again that there is no correlation between the results in a very active atmosphere like SST and a more passive atmosphere like outdoor exposure. While we see red rust in the scratch after 6 months of outdoor exposure which is below typical corrosion requirements, we do not see any red rust in the SST after 1000 h (1.5 months) which is a relatively high requirement from typical automotive specifications.

Therefore, while it is well known that the environment has a direct impact on the corrosion protection mechanism, fulfilling corrosion requirements from short-term simulation tests, as required in various industries, is no guarantee for long-lasting corrosion protection during outdoor weathering. The planning and interpretation of accelerated tests and natural exposure results are thus crucial.

3.2 | ICP-MS results

Using an ICP-MS flow cell approach on steel panels coated with zinc flake systems, we now provide further insight into the corrosion mechanism for explaining the differences in the various standardised corrosion tests described above. We are able to study different dissolution rates of the included metals.

When using mixed and alloyed zinc flake systems (Table 2a,b), there can be overlapping effects of the individual flakes on corrosion rates. Therefore, to decouple the contributions of the different flakes we now use single zinc and single ZnAlMg flake systems (Table 2c,d).

First, Figure 3 shows the results of the dissolution rates of single flake systems. We have conducted a 40 min

open circuit potential (OCP) measurement coupled to the ICP-MS with a 1 mM NaCl electrolyte at a pH-value of 7. Further, the activity during corrosion protection can be obtained by comparing (a and c) undamaged coating systems and (b and d) samples with a 1 mm scratch which goes through to the base metal.

Even though the NaCl concentration used is much lower than, for example, in SST, we assume that the basic corrosion reactions occur in a similar way on the surface, which can be easily detected due to the very high sensitivity of ICP-MS. The ICP-MS setup is not suitable for high salt concentrations as in SST (800 mM), which is why we worked with a maximum concentration of 80 mM in the further experiments, which corresponds to the NaCl content from the ACT II test (Table 1).

In terms of the zinc corrosion, two effects can clearly be derived from Figure 3. First, the pure zinc flake coating (a and b) shows a higher zinc dissolution current in both sample conditions compared to the ZnAlMg system (c and d). In panel a, we see that the current density at the intact surfaces for the pure zinc (24 μA/cm^2) is twice as high as the rate of dissolution for the ZnAlMg alloy in c (12 μA/cm^2). For the scratched samples, in b, the surface with pure zinc (70 μA/cm^2) shows almost three times the current density of the alloyed system in d (27 μA/cm^2). Even considering the slightly lower zinc contents in the single ZnAlMg system compared to the single zinc system, once normalised to the same equivalent zinc content in Figure 3c,d, the current density increases only marginally (to 14 and 30 μA/cm^2, respectively).

Second, though a significant area of the analysed surface is the blank steel in b and d, we observe higher current densities of zinc dissolution after applying a 1 mm scratch. Here the zinc is cathodically active and protects the steel sacrificially from corroding (i.e., no Fe dissolution detected). This effect is much more pronounced on the samples with pure zinc, which indicates that this system more actively dissolves compared to the ZnAlMg system.

In contrast to the cathodically protective surfaces, Figure 4 shows that we can observe Fe-dissolution when using a passive coating system like an epoxy-based cathodic dip coating with a 1 mm scratch or using uncoated S235JR steel panels. This proves that we can detect elements with the ICP-MS method, which are deposited on the surface as insoluble corrosion products such as red rust or white rust. This is further supported by the fact that the scribed sample with the passive cathodic dip coating shows red rust in the scribed area after the 30 min OCP test (Figure 4).

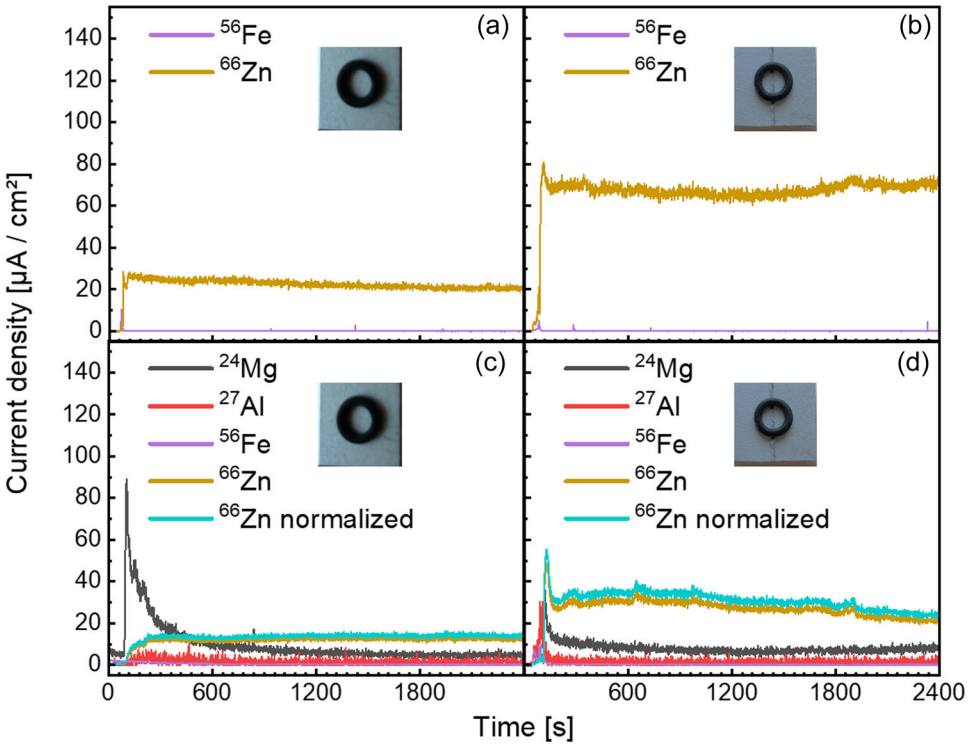

FIGURE 3 Inductively coupled plasma mass spectrometry (ICP-MS) measurements (40 min OCP) with 1 mM NaCl electrolyte with different flake coatings with and without defects. (a) Pure zinc flake coating (intact); (b) Pure zinc flake coating (1 mm scratch); (c) pure ZnAlMg alloy flake coating (intact); (d) pure ZnAlMg alloy flake coating (1 mm scratch). The Zn normalised line in c and d is normalised to the equivalent zinc content of the single zinc flake system.

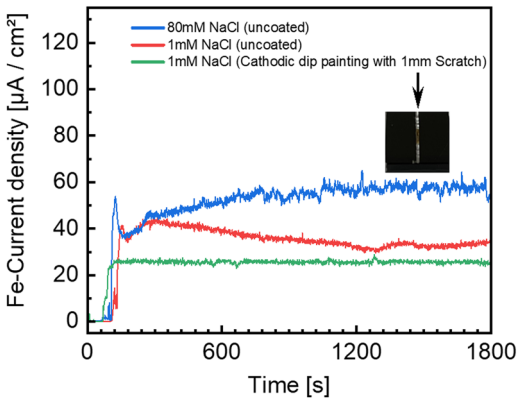

FIGURE 4 Fe current densities on an S235JR sample coated with a passive epoxy-based cathodic dip coating with a 1 mm scratch and Fe current densities on uncoated steel panels (S235JR) with two different electrolyte concentrations.

In addition, in Figure 3c,d, a magnesium dissolution can be observed from the alloyed flake in the initial seconds, which, however, drops to a significantly lower level within 10 min. Aluminium does not dissolve, which is consistent with the Pourbaix diagram, as it is passive at pH 7.

These data suggest that the surface oxides formed moderate the dissolution rate. Regarding the different surface oxide species, the zinc oxide retards the dissolution to a lesser extent compared to the magnesium and aluminium oxides, which appear to slow down the dissolution kinetics of the sacrificial zinc corrosion more effectively.

Regarding the stability of the coating and its continued cathodic protection, there is a further interface that should be considered between the newly formed oxides and the binder matrix. Hausbrand et al. found that the interface between the metal oxides and a polymer binder is highly relevant to cathodic delamination. Due to the negative potential of polymer-coated $MgZn_2$, which is a main phase in ZnAlMg, cathodic delamination is completely inhibited in these coatings, thus influencing also the cathodic corrosion protection.[42] The system used here, with an inorganic matrix is more porous than the polymer systems, contains a high concentration of metallic flakes (Table 2) to maximise the contact between them. Although we have not explored the direct influence of the interface between the binder and oxide specifically in these experiments, and do not see macroscopic delamination as a result of the changes oxide growth causes at this interface, it should be considered that it could also influence the dissolution kinetics.

In this wet and saline environment, the two tested substrates show no Fe dissolution which proves that the base metal in the scratched area is protected, irrespective of the zinc dissolution kinetics. These findings are in line with the results from Figure 2a1,a2. Both the mixed system and the alloyed system can therefore provide cathodic protection in this salt-rich environment, as the zinc flakes are actively dissolving. Also, the more passive behaviour of the alloyed system fits to the outdoor exposure results from Figure 2d2,e2. Here, the alloyed system with the ZnAlMg flakes embedded in the binder matrix is probably not activated sufficiently to provide cathodic protection.

Due to the predominant role of zinc for corrosion protection, we have further analysed the cathodic corrosion behaviour in Figure 5. In addition to the pure zinc flake, we have further included the two test recipes of zinc flake coatings which are already described previously (Table 2a,b). Figure 5a shows that for undamaged coatings the zinc current densities are almost equal for the mixed system and the pure zinc flake system. The dissolution rate of the pure ZnAlMg system is equal to the alloyed system, owing to the predominant flake type in the test recipe.

In the event of damage being applied, the Zn-current densities in Figure 5b split up and again confirm the different zinc dissolution activities of the coating systems. The single flake system made from pure ZnAlMg forms the lower extreme, whereas the other coating systems increase their Zn current densities according to the content of pure zinc flake. Hence the single flake system with pure zinc and the mixed system show the highest Zn current densities.

Figure 2 already indicates the influence of different corrosive atmospheres on the corrosion mechanism of zinc flake systems. Thus we subsequently conducted ICP-MS measurements with different electrolytes to further assess the impact of salinity on the zinc dissolution rates. The findings are plotted in Figure 5c for the electrolytes MilliQ water, 1 mM NaCl and 80 mM NaCl. One can directly see that the nonconductive environment with MilliQ water leads to the same zinc dissolution rate, irrespective of whether there is damage or not. The presence of a 1 mm scratch does not result in any significantly elevated zinc dissolution.

In contrast, in 1 mM NaCl electrolyte, a clear difference is visible between the scratched and the ideal state. When damaged, the zinc dissolves much faster, which leads to the cathodic protection of the steel. Higher concentrations at 80 mM NaCl solutions further increase the zinc current density.

In general, these findings confirm the results of the corresponding corrosion tests (Figure 2), where the mixed zinc flake system with mainly zinc flakes shows an active behaviour and tends to form white rust in a saline environment like the salt spray test. The alloyed system shows higher passivity which can be seen in the

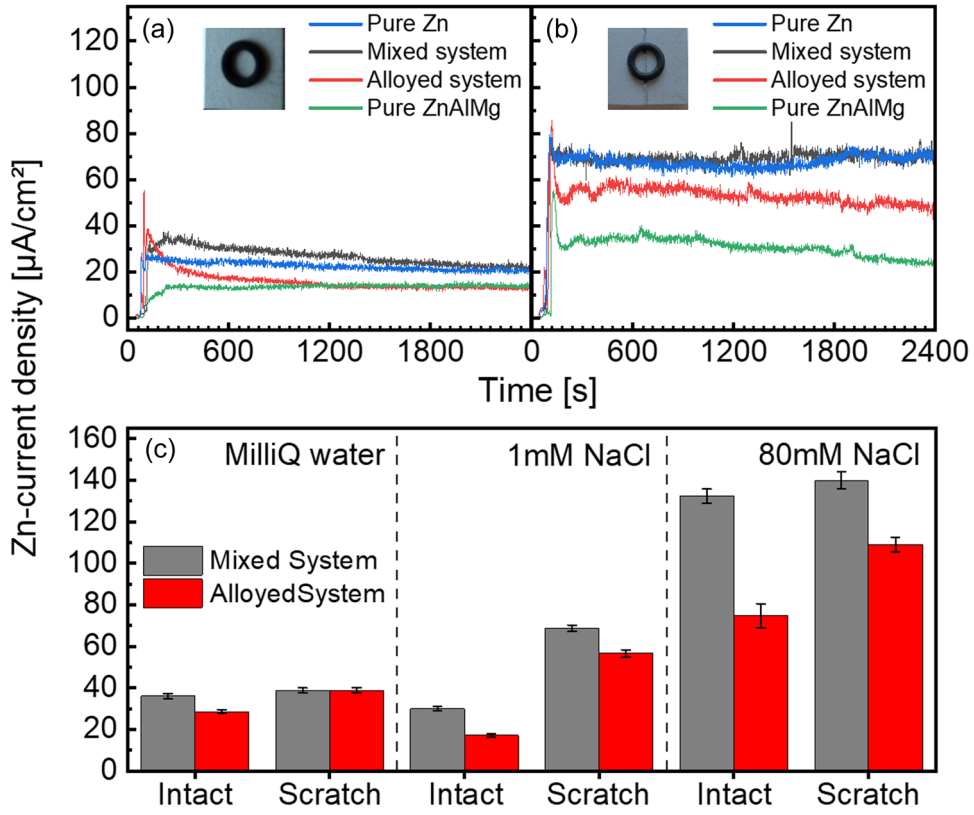

FIGURE 5 Inductively coupled plasma mass spectrometry (ICP-MS) measurements (40 min OCP) with (a) intact zinc flake coatings and (b) predamaged zinc flake coatings with 1 mm scratch with a 1 mM NaCl electrolyte. (c) Average Zn-current density from OCP measurements with different electrolytes with increasing salt concentrations (normalised to zinc content from single zinc flake system).

lower zinc dissolution and also in the results of the corrosion tests with a clear tendency to form less white rust. Further, with all tested electrolytes no Fe-dissolution can be detected which proves the cathodic corrosion protection capability of zinc flake systems.

When comparing ICP-MS results and outdoor exposures (experiments d/e in Figure 2), the data seems to suggest that a certain level of dissolution of the transiently forming passive film is necessary to ensure cathodic protection via zinc dissolution across the oxide which is also in line with our expectations. In particular, the more passive alloyed system shows red rust formation under mild outdoor exposure, while the more actively dissolving mixed system prevents red rust formation during outdoor exposure, which is also indicated in other studies on ZnAl coatings.[43]

Hence, the assumed formation of the oxides within the coating moderates the rate of zinc dissolution, making the alloy more resistant to the aggressive salt-rich environments and the mixed system, with its higher Zn-dissolution rates, ideally protects the underlying steel well in milder conditions. Therefore, it is necessary to tune the coating composition to the environment in which protection is required.

At this point, it should be mentioned that the specific situation of zinc flakes embedded in a binder system (here: relatively porous titanates) can influence the activity of the flakes present. Several studies have shown that the cathodic protection in inorganic binders is significantly greater than in organic epoxy systems, which is presumably due to the fact that the porous structure of the titanates allows better contacting of the flakes with each other and the easier penetration of water to provide better overall conductivity and thus better cathodic protection.[12,44,45] Further development of customised zinc flake coatings and alloy systems for specific environments will enable tailored coatings with superior performance.

4 | CONCLUSIONS

In summary, the presented data indicate that the environment and in particular how salt affects the sacrificial zinc dissolution rate is a key moderator for performance of zinc flake coatings. Our data indicate that the native oxide stability of the various alloys controls the zinc dissolution.

Although accelerated laboratory corrosion tests like salt spray tests and cyclical corrosion tests are commonly used to predict the behaviour of coatings in real-life conditions, we observed discrepancies between all laboratory corrosion tests and the outdoor exposure tests. The chloride concentration of the media under these various conditions appears to be a key aspect moderating the dissolution rate and hence sacrificial zinc dissolution. ICP-MS flow cell experiments further support the specific zinc dissolution of current densities under different electrolytes and sample conditions.

The detailed findings of this study can be summarised as follows:

- Accelerated corrosion tests have limitations in predicting the general corrosion behaviour of cathodically protective surfaces such as zinc flake coatings. However, with a careful interpretation of accelerated laboratory tests, in terms of expected chloride exposure in the field, various situations can be predicted.
- The mixed flake system which consists of zinc and aluminium flakes shows a higher zinc dissolution rate compared to the alloyed flake system. This agrees with the increased formation of white rust of the mixed zinc flake system in laboratory tests.
- Higher zinc dissolution rates are necessary to build up a good corrosion protection in outdoor exposures with typically low salt concentrations.
- The alloyed system, with ZnAlMg, shows a more pronounced passive behaviour, with a factor of 2–3 lower passive zinc dissolution currents. In salt-rich environmental conditions (e.g., SST and ACT II test) this has the advantage of suppressing the formation of visible white rust, while still delivering cathodic corrosion protection.
- Conversely, mild environments without salt lead to less zinc dissolution, and hence lower cathodic corrosion protection, which results in a corrosive attack of the base metal (red rust).

Where the ZnAlMg is present, the suppressed zinc dissolution rate appears to derive from the passivation of the alloy by an effective oxide barrier. Although we believe the oxide to have the greatest influence, its interaction with the binder at the flake-binder interface could also change the dissolution kinetics for different alloys. Future research must focus on how oxide growth mediates zinc dissolution and cathodic corrosion protection in different environmental conditions. Furthermore, the influence of the binder and the impact of topcoats on the corrosion mechanism should be integrated into future studies.

ACKNOWLEDGEMENTS

This work was performed within the framework of cooperation between Dörken Coatings GmbH & Co. KG and the Applied Interface Physics group of the TU Wien. Dominik Dworschak and Lukas Kalchgruber are thanked for the introduction and support of the ICP-MS experiments. Gerhard Reusmann, Christos Tselebidis and Christian Rabe are thanked for critically reading and discussing the manuscript. We also thank the University Service Centre for Transmission Electron Microscopy, Vienna University of Technology, Austria for carrying out the SEM measurements. The authors acknowledge the TU Wien University Library for financial support through its Open Access Funding Program. Open access funding provided by KEMO - Technische Universitat Wien.

DATA AVAILABILITY STATEMENT

Raw and processed data are available from the corresponding author via www.repositum.tuwien.ac.at upon reasonable request.

ORCID

Laura L. E. Mears https://orcid.org/0000-0001-7558-9399
Markus Valtiner https://orcid.org/0000-0001-5410-1067

REFERENCES

[1] B. Chatterjee, *Jahrb. Oberfl* **2017**, *72*, 1.
[2] B. Oleksiak, K. Kołtało, R. Poloczek, *Metalurgija* **2021**, *60*, 162.
[3] P. Wynn, *Trans IMF* **2003**, *81*, B16.
[4] H. Ren, H. Benz, O. Chimal, M. Corral, Y. Zhang, D. Jaramillo, H. Zoz, *Proc. Korean Powder Metallurgy Inst. Conf.*, pp. 975, **2006**.
[5] A. Bariska, T. Kleyer, *JOT* **2019**, *59*, 34.
[6] *DIN EN ISO 10683: Fasteners – Nonelectrolytically applied zinc flake coating systems (ISO 10683:2018)*, **2018**.
[7] C. Lenzmann, *JOT* **2019**, *59*, 46.
[8] A. Kalendová, *Prog. Organic Coat.* **2003**, *46*, 324.
[9] S. Yurtdaş, İ. Umut, B. Tanrikulu, C. Kiliçaslan, M. B. Toparli, *Sakarya Univ. J. Sci.* **2021**, *25*, 867.
[10] R. Knott, J. Schneider, *JOT* **2012**, *52*, 60.
[11] S. K. Dwivedi, M. Vishwakarma, *Int. J. Hydrogen Energy* **2018**, *43*, 21603.
[12] M. Zubielewicz, E. Langer, A. Królikowska, L. Komorowski, M. Wanner, K. Krawczyk, L. Aktas, M. Hilt, *Prog. Organic Coat.* **2021**, *161*, 106471.
[13] H. Wiegand, K.-H. Kloos, W. Thomala, *Schraubenverbindungen: Grundlagen, Berechnung, Eigenschaften, Handhabung*, Springer-Verlag, Berlin, **2013**.
[14] *ICS Handbuch: Industrielle Schraubmontage* Deutscher Schraubenverband e.V., Hagen **2007**.
[15] N. LeBozec, N. Blandin, D. Thierry, *Mater. Corros.* **2008**, *59*, 889.
[16] *DIN EN ISO 9227: Korrosionsprüfungen in künstlichen Atmosphären – Salzsprühnebelprüfungen (ISO 9227:Juli 2017)*, Beuth Verlag, **2017**.

[17] F. Altmayer, *Plating Surface Fin.* **1985**, *72*, 36.
[18] *DIN EN ISO 6270-2: Beschichtungsstoffe - Bestimmung der Beständigkeit gegen Feuchtigkeit - Teil 2: Kondensation (Beanspruchung in einer Klimakammer mit geheiztem Wasserbehälter) (ISO 6270-2:2017)*, Beuth Verlag, **2018**.
[19] *VDA 233-102: Zyklische Korrosionspr¨ufung von Werkstoffen und Bauteilen im Automobilbau/Cyclic Corrosion Testing of Materials and Components in Automotive Construction (Version 06/2013)*, Verband der Automobilindustrie e. V. (VDA), **2016**.
[20] *PV 1210: Body and Add-On Parts/Hang-On Parts Corrosion Test*, Volkswagen, **2016**.
[21] *PV 1200: Fahrzeugteile Prüfung der Klimawechselfestigkeit* (80°C/-40°C), Volkswagen, **2019**.
[22] *PV 1209: Add-On Parts/Hang-On Parts with a Zinc or Zinc Alloy Coating and Aluminium Add-On Parts/Hang-On Parts (e.g., Heat Exchanger, Refrigerant Line) Corrosion Test (Environmental Corrosion Cycle Test*, Volkswagen, **2016**.
[23] *STD 423-0014: Accelerated Corrosion Test: Atmospheric Corrosion*, Volvo Group, **2015**.
[24] *VCS 1027,1449: Accelerated Corrosion Test, Version II – ACT II Cyclic Atmospheric Corrosion Test with Salt Load*, Volvo Car Corporation, **2014**.
[25] *AA-0224: Korrosionswechseltest/Cyclic Corrosion Test*, BMW Group, **2015**.
[26] *GMW14872: Cyclic Corrosion Laboratory Test*, GM, **2013**.
[27] T. H. Muster, I. S. Cole, *Corros. Sci.* **2004**, *46*, 9.
[28] C. Köse, *PhD thesis*, Universität Stuttgart, Stuttgart **2019**.
[29] R. Howard, S. Lyon, J. Scantlebury, *Prog. Organic Coat.* **1999**, *37*, 91.
[30] S. S. Pathak, M. D. Blanton, S. K. Mendon, J. W. Rawlins, *Corros. Sci.* **2010**, *52*, 1453.
[31] N. LeBozec, D. Thierry, A. Peltola, L. Luxem, G. Luckeneder, G. Marchiaro, M. Rohwerder, *Mater. Corros.* **2013**, *64*, 969.
[32] M. Babutzka, *Neue Erkenntnisse zur Deckschichtbildung von Zink an der Atmosphäre*, Shaker Verlag, Düren, **2020**.
[33] S. O. Klemm, A. A. Topalov, C. A. Laska, K. J. Mayrhofer, *Electrochem. Commun.* **2011**, *13*, 1533.
[34] A. K. Schuppert, A. A. Topalov, I. Katsounaros, S. O. Klemm, K. J. Mayrhofer, *J. Electrochem. Soc.* **2012**, *159*, F670.
[35] K. Ogle, S. Weber, *J. Electrochem. Soc.* **2000**, *147*, 1770.
[36] D. Dworschak, C. Brunnhofer, M. Valtiner, *ACS Appl. Mater. Interf.* **2020**, *12*, 51530.
[37] V. Großmann, N. Johanterwage, N. JoseSimoes, N. Matthee, H. Mertens, K. Owczarek, G. Reusmann, M. Roth, European Patent EP 2 933 355 B1, **2019**.
[38] V. Clerici, A. Wilhelmi, J. Yamashita, *International Patent WO 01/85854 A1*, **2001**.
[39] T. Griebling, personal communication, **2022**.
[40] N. LeBozec, D. Thierry, D. Persson, C. K. Riener, G. Luckeneder, *Surf. Coat. Technol.* **2019**, *2019*, 897.
[41] R. Krieg, A. Vimalanandan, M. Rohwerder, *J. Electrochem. Soc.* **2014**, *161*, C156.
[42] R. Hausbrand, M. Stratmann, M. Rohwerder, *J. Electrochem. Soc.* **2008**, *155*, C369.
[43] Z. Panossian, L. Mariaca, M. Morcillo, S. Flores, J. Rocha, J. Peña, F. Herrera, F. Corvo, M. Sanchez, O. Rincon, G. Pridybailok, J. Simancas, *Surf. Coat. Technol.* **2005**, *190*, 244.
[44] S. Shreepathi, P. Bajaj, B. Mallik, *Electrochim. Acta* **2010**, *55*, 5129.
[45] N. Hammouda, H. Chadli, G. Guillemot, K. Belmokre, *Adv. Chem. Eng. Sci.* **2011**, *1*, 51.

How to cite this article: F. Feldmann, L. L. E. Mears, M. Roth, M. Valtiner, *Mater. Corros.* **2023**, 74, 1148–1158. https://doi.org/10.1002/maco.202213719